Supplementary Information for

Flexible MXene-sponge piezoresistive array for multi-point hand-pressure monitoring in badminton forehand smashes

S1. Detailed fabrication procedure of the MXene-sponge piezoresistive array

S1.1 Materials

Commercial Ti_3C_2 MXene aqueous colloidal dispersion (30 mg mL^{-1}), melamine sponge sheets (nominal thickness 2 mm), polyimide (PI) films (50 μm), isopropanol (IPA, 0.1 mol L^{-1}), anhydrous ethanol, conductive silver paste, disposable plastic droppers, and polyimide adhesive tape were used as listed in the main text. Deionized (DI) water (resistivity ≥ 18.2 MΩ·cm) was used throughout all procedures.

All chemicals and substrates were used as received unless otherwise specified. Before use, bottles of Ti_3C_2 dispersion were gently shaken and sonicated for 10 min in an ultrasonic bath to redisperse any settled MXene flakes and obtain a visually homogeneous colloid.

S1.2 Pre-treatment of melamine sponge

1. Cutting

Melamine sponge sheets were cut into circular discs with a nominal diameter of 6.5 mm and thickness of 2.0 mm using a precision blade and a circular cutting die. Care was taken to keep the cutting edge sharp to avoid crushing or deforming the porous structure.

2. Cleaning

The sponge discs were transferred into a glass beaker containing DI water and gently agitated on an orbital shaker for 2 h to remove surface dust and processing residues. The discs were then moved into a fresh beaker containing 0.1 mol L^{-1} IPA and soaked for another 2 h with the same gentle agitation.

This DI–IPA soaking sequence was repeated twice in total (i.e., two cycles of DI water followed by IPA), and the cleaning solutions were replaced in each step.

3. Drying

After cleaning, the discs were removed with tweezers, gently blotted with lint-free tissue to remove excess liquid, and placed flat on a piece of heat-resistant PI film. The samples were dried in a vacuum oven at 80 °C for 1 h, then allowed to cool to room temperature. This drying step was repeated four times to ensure complete removal of residual solvents and moisture.

S1.3 Dip-coating of melamine sponge with MXene

1. Preparation of coating bath

A total of 30 mL of Ti_3C_2 MXene colloidal dispersion (30 mg mL^{-1}) was poured into a clean 50 mL glass beaker to form the coating bath. Immediately prior to coating, the dispersion was sonicated for 5–10 min to ensure uniform particle distribution.

2. Vacuum-assisted impregnation

Dried sponge discs were fully immersed in the MXene dispersion. The beaker was then placed in a vacuum desiccator and evacuated until vigorous bubbling from the sponge ceased (typically within several minutes). The vacuum was maintained for a total of 20 min to facilitate complete removal of trapped air and thorough infiltration of the dispersion into the sponge

network. Vacuum was released slowly to avoid splashing and disturbance of the discs.

3. Drying

After impregnation, the coated sponge discs were removed from the bath and placed on PI film to drain excess liquid. The discs were subsequently transferred into a vacuum oven and dried at 80 °C for 3 h until visually dry.

4. Repeated coating cycles

The impregnation and drying steps described above were repeated six times in total. After each drying cycle, the discs were re-immersed in the MXene dispersion for 20 min and then dried again at 80 °C for 3 h. During each cycle, the discs were gently flipped to promote uniform coating on all sides.

After the final cycle, the MXene–sponge composites were allowed to cool to room temperature and stored in a desiccator before device assembly. Under these conditions, the composites remained stable in appearance and electrical response over the time frame of the experiments.

S2. Fabrication of interdigitated electrodes and sensor assembly

S2.1 Cleaning and preparation of PI substrates

Polyimide films (50 μm thickness) were cut into rectangular pieces slightly larger than the designed electrode area. The PI pieces were sequentially rinsed with anhydrous ethanol and DI water, gently wiped with lint-free tissue, and air-dried at room temperature. To further remove residual moisture, the cleaned PI substrates were placed in a drying oven at 60 °C for 10–15 min and then cooled to room temperature in a dust-free environment.

S2.2 Screen-printing of interdigitated electrodes

1. Electrode pattern design

A circular interdigitated electrode (IDE) pattern was designed using CAD software. The active area comprised four pairs of interdigitated fingers arranged in a circular geometry. The design parameters were: finger width w=0.4 mm, finger spacing d=0.4 mm, overlap length $l_o \approx$ 6.2 mm, and number of finger pairs n = 4. These dimensions were chosen to provide a dense, symmetric current path beneath the MXene–sponge disc, supporting high sensitivity and fast response.

2. Screen preparation and printing

The CAD pattern was transferred to a 300-mesh stainless-steel screen using a standard photoresist process. During printing, PI substrates were fixed on the vacuum printing table to prevent movement. Conductive silver paste was dispensed onto the screen, and a polyurethane squeegee was drawn across the screen at a constant speed and angle (~45°) to print the electrode pattern onto the PI surface in a single pass.

3. Curing

Immediately after printing, the PI films with wet silver paste were placed in a vacuum oven and thermally cured at 130 °C for 20 min to solidify the electrodes and improve adhesion. After curing, the electrodes were allowed to cool to room temperature and visually inspected under an optical microscope to ensure that all fingers were continuous and free of pinholes.

4. Cutting

The printed PI films were trimmed with a precision blade so that each piece contained one

complete circular electrode and a pair of terminal pads for electrical connection.

S2.3 Assembly of MXene–sponge sensor units

1. Mounting of MXene–sponge discs

A small amount of uncured conductive silver paste was applied to the active area of the interdigitated electrode. A single MXene–sponge disc was gently placed on top, centered over the circular IDE region. Light pressure was applied with tweezers to ensure intimate mechanical contact without deforming the sponge. The assembly was then cured again at 80–100 °C for 20–30 min to secure the disc and allow the paste to fully set.

2. Electrical connections

Two thin aluminum leads were attached to the terminal pads of the electrode using conductive silver paste. After curing, the joints were inspected to confirm mechanical robustness and low electrical contact resistance.

3. Encapsulation

To protect the device from mechanical damage and environmental influences while preserving flexibility, the entire sensor (MXene–sponge disc, electrode region, and lead junctions) was encapsulated between layers of polyimide adhesive tape. The upper and lower tape layers were pressed together from the center outward to avoid trapping air bubbles. Excess tape around the edges was trimmed with a blade to achieve a compact, lightweight device.

The final flexible MXene–sponge piezoresistive sensor unit had a mass of approximately 0.1 g and could be bent to conform to curved surfaces such as a badminton racket handle.

S3. Electrical characterization and calibration of the MXene–sponge sensors

S3.1 Quasi-static pressure–response measurements

1. Test platform

A custom high-precision testing platform was assembled, consisting of a motorized linear actuator, a load cell for normal force measurement, a source–measure unit, and a LabVIEW-based control and acquisition system. Sensor units were mounted on the movable stage of the linear actuator using double-sided adhesive tape, with the sensing surface oriented upward. The load cell was aligned coaxially above the sensor to apply normal compressive loads.

2. Instrument settings

A Keithley 2611B digital source meter was used to supply a constant voltage and measure the corresponding current through the sensor. Unless otherwise specified, the maximum output voltage of the system was set to 20 V, with an operational voltage range of −1 to 1 V and a current range up to 1 mA. The sampling interval was chosen such that each loading and unloading process was recorded with sufficient temporal resolution for subsequent analysis.

3. Pressure loading protocol

For quasi-static characterization, the actuator was programmed to apply a series of discrete normal pressures to the sensor over the range 1.1–266 kPa. At each target pressure, the actuator advanced until the load cell reading reached the desired value, then held this load for a fixed dwell time (e.g., 30–60 s) while the current–time (I–T) signal was recorded. The procedure was repeated for increasing pressure levels to obtain the full pressure–current response.

For selected pressures within 0–22.2 kPa and 22.2–266 kPa, current–voltage (I–V) curves

were measured by sweeping the applied voltage between −1 and 1 V at a constant rate while maintaining the normal pressure constant.

4. Sensitivity calculation

The relative change in current, $\Delta I/I_0$, was calculated with respect to the baseline current at negligible load. Sensitivity S was defined as the slope of $\Delta I/I_0$ versus applied pressure P in each linear region and obtained by piecewise linear fitting. Low-pressure (0–22.2 kPa) and high-pressure (22.2–266 kPa) segments were fitted separately to extract corresponding sensitivities and coefficients of determination (R^2).

S3.2 Dynamic response, stability, and frequency tests

1. Response and recovery time

To evaluate dynamic response, the sensor was subjected to a square-wave pressure input at a representative pressure level (e.g., 3.36 kPa). The actuator alternated between "no load" and "target load" at a predefined period while the I–T signal was recorded. Response time was defined as the time for the current to reach 90% of its steady-state value after load application, and recovery time was defined analogously after load removal.

2. Cyclic stability

Repeated loading–unloading cycles were applied at a fixed pressure to assess repeatability and long-term stability. The amplitude and shape of the current signal over extended cycling (hundreds to thousands of cycles) were examined to confirm that no significant drift or degradation occurred.

3. Frequency and speed dependence

The actuator speed and excitation frequency were systematically varied over a practical range to simulate different hand-motion rates. At each condition, I–T curves were recorded and compared to evaluate whether the sensor response remained stable and consistent across frequencies and loading speeds. Periodic pressure tests were performed to obtain synchronized pressure–time (P–T) and current–time (I–T) curves, verifying real-time tracking of dynamic loads.

S4. Badminton forehand smash testing protocol with the sensor array

S4.1 Sensor placement on the racket handle

Six MXene–sponge sensor units were mounted on the surface of a standard badminton racket handle to monitor palmar pressure at key contact sites: the thumb, index finger, middle finger, ring finger, little finger, and heel of the palm. The handle was first cleaned with ethanol and allowed to dry completely.

The approximate locations of these palmar landmarks were determined by asking a player to grip the racket in their usual forehand smash grip and marking the regions of maximum contact. The six sensors were then affixed to the marked regions with double-sided adhesive tape and further secured with a thin overwrap of sports tape to ensure firm contact while minimally affecting grip feel and racket balance.

S4.2 Participants and warm-up

This study recruited badminton players of varying skill levels (elite, intermediate, and beginner) to practice forehand smashes using rackets equipped with sensors. All experimental

procedures involving human subjects were approved by the institution's ethics committee, and written informed consent was obtained from all participants. A total of 30 male badminton players participated in the experiment (10 national first-class athletes, 10 national second-class athletes, and 10 amateur athletes). Their detailed information is summarized in Supplementary Table S1.

Table S1. Anthropometric characteristics and playing level of the participants

Name	Age (years)	Height (m)	Body mass (kg)	BMI ($kg \cdot m^{-2}$)	Playing level
BXX	20	1.84	72	21.27	National first-class athlete
CX	19	1.85	75	21.91	National first-class athlete
YXX	24	1.80	83	25.62	National first-class athlete
LXXX	19	1.85	75	21.91	National first-class athlete
MXX	24	1.83	70	20.90	National first-class athlete
YXX	18	1.84	77	22.74	National first-class athlete
XXX	19	1.88	79	22.35	National first-class athlete
LXX	21	175	62	20.24	National first-class athlete
ZXX	22	175	77	25.14	National first-class athlete
WXX	22	188	88	24.90	National first-class athlete
ZXX	21	194	80	21.26	National second-class athlete
LXX	19	1.83	72	21.50	National second-class athlete
ZXX	23	1.72	75	25.35	National second-class athlete
SXX	22	1.78	72	22.72	National second-class athlete
ZX	23	1.78	76.5	24.14	National second-class athlete
LX	23	1.75	72	23.51	National second-class athlete
WX	23	1.82	73	22.04	National second-class athlete
HXX	23	1.80	75	23.15	National second-class athlete
YXX	22	1.78	72	22.72	National second-class athlete
LXX	22	1.81	70	21.37	National second-class athlete
FX	23	170	68	23.53	Amateur player
FXX	19	170	67	23.18	Amateur player

ZXX	19	172	65	21.97	Amateur player
HXX	21	172	69	23.32	Amateur player
SXX	20	175	66	21.55	Amateur player
LXX	19	178	71	22.41	Amateur player
YXX	21	171	63	21.54	Amateur player
CXX	19	176	69	22.28	Amateur player
HXX	23	180	75	23.15	Amateur player
GXXX	22	180	76	23.46	Amateur player

Before data collection, each player completed a standardized warm-up consisting of 5–10 min of light aerobic activity, dynamic stretching of the upper limbs and trunk, and several sub-maximal practice swings to familiarize themselves with the instrumented handle.

S4.3 Forehand smash test protocol

1. Task instructions

Participants were instructed to perform forehand overhead smashes using their preferred technique while gripping the instrumented racket as naturally as possible. They were asked to strike shuttles directed to a consistent hitting zone, aiming for maximal but controlled stroke quality rather than simply maximum effort.

2. Trial organization

For each participant, multiple forehand smashes were recorded to obtain representative pressure–time profiles. Trials in which the participant mis-hit the shuttle, lost balance, or clearly deviated from their usual technique were marked and excluded from analysis. Only technically successful smashes with consistent contact location were retained.

3. Phase definition

The smash motion was conceptually divided into four phases for subsequent analysis:

(1) turn-and-backswing;

(2) accelerative downswing;

(3) impact;

(4) follow-through.

Phase boundaries were identified from synchronized shuttle–racket contact timing and characteristic features in the pressure–time curves (e.g., onset of rapid pressure rise and the peak around impact). The experimental setup of the badminton forehand smash test is illustrated in Figure S1.

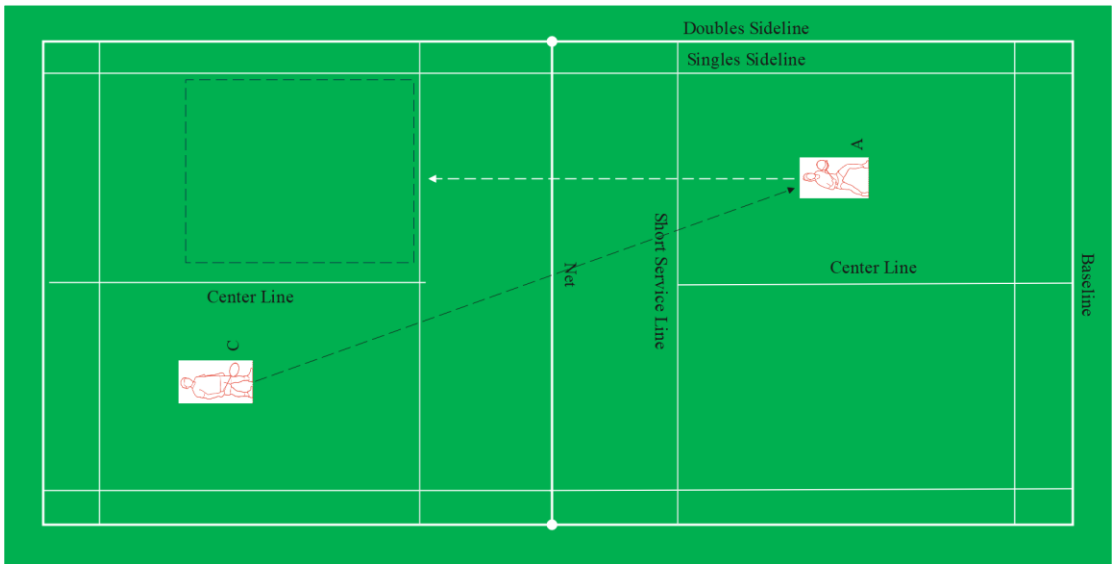

Figure S1. Schematic diagram of the badminton forehand smash test. Participant A performs a forehand overhead smash from the right rear singles court. Feeder C stands in the left rear court and sends a lifted shuttlecock toward A (diagonal dashed line). Participant A hits a forehand smash across the net, aiming at the designated target area in the opponent's rear court (dashed rectangle), as indicated by the horizontal dashed arrow.

S4.4 Data acquisition and processing

During forehand smash tests, all six sensors were connected to the electrical testing system described in Section S3. A constant bias voltage was applied, and the current from each sensing channel was recorded simultaneously throughout each stroke. The on-court experimental setup and real-time data acquisition interface are shown in Supplementary Figure S2.

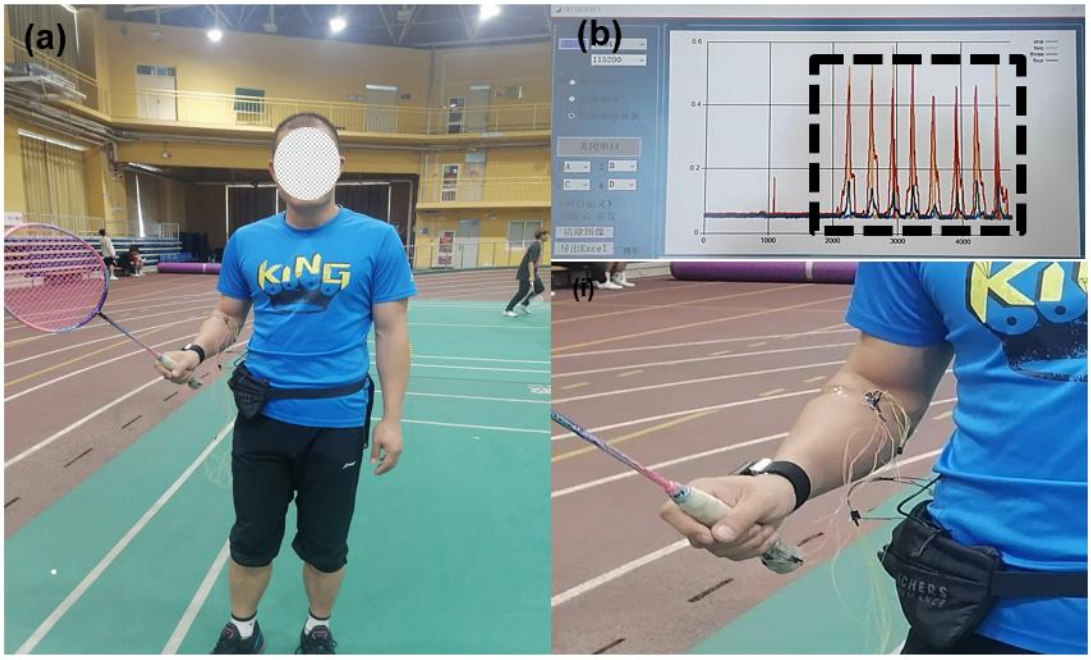

Figure S2. Experimental setup for the badminton forehand smash test with the MXene–sponge sensor array. (a) A participant holding the instrumented racket on the badminton court, with the portable data

acquisition unit fixed at the waist. (b) Close-up view of the racket handle with attached MXene–sponge sensors and the real-time current signals displayed on the computer interface.

Raw current–time data were first visually inspected to remove trials with obvious artifacts. For each valid trial, the current was baseline-corrected by subtracting the mean value during the pre-swing period. If necessary, a low-pass filter was applied to remove high-frequency noise without distorting the main waveform.

For each palmar site and participant, characteristic parameters such as peak current, time-to-peak, and curve regularity within each phase were extracted and used to compare loading patterns across sites and skill levels, as presented in the main text.